Catalysis Today 138 (2008) 253–259

Contents lists available at ScienceDirect

Catalysis Today

journal homepage: www.elsevier.com/locate/cattod

Development of catalysts for hydrogen generation from hydride compounds

Valentina I. Simagina [a,*], Pavel A. Storozhenko [b], Olga V. Netskina [a], Oksana V. Komova [a], Galina V. Odegova [a], Yury V. Larichev [a], Arcady V. Ishchenko [a], Anna M. Ozerova [a,c]

[a] Boreskov Institute of Catalysis SB RAS, Pr. Akademika Lavrentieva 5, Novosibirsk 630090, Russia
[b] State Research Institute of Chemistry and Technology of Organoelement Compounds, Sh. Entuziastov 38, Moscow 111123, Russia
[c] Novosibirsk State University, Pirogova street, 2, Novosibirsk 630090, Russia

ARTICLE INFO

Article history:
Available online 7 July 2008

Keywords:
Sodium borohydride
Ammonia borane
Hydrogen generation
Hydrolysis
Catalyst

ABSTRACT

Catalytic hydrolysis of $NaBH_4$ and NH_3BH_3 has been studied. It was shown that the nature of the support and the active component of the catalyst affect the H_2 generation rate. Despite similar sizes of rhodium particles formed on the surface of different supports (γ-Al_2O_3, TiO_2, carbon), their reactivity is different. Rh/TiO_2 with low rhodium concentration (1 wt.%) is the most active catalyst both in the hydrolysis of $NaBH_4$ and NH_3BH_3. The obtained results show that the rhodium chloride interaction with titania determines the reactivity of rhodium particles formed under action of $NaBH_4$ medium. TEM, DRS UV–vis and XPS were used to characterize the catalysts.

1. Introduction

Creation of independent, compact and safe energy sources became possible due to development of low-temperature proton exchange membrane fuel cells (PEM FC). However, the use of hydrogen (H_2) requires solution of an important problem related to development of a compact system for its storage and generation because at ambient conditions hydrogen is a gas with a very low density (0.000089 g/cm^3) [1].

Chemical hydrides are very prospective materials for hydrogen supply to portable fuel cells at ambient temperature (−20, ..., +55 °C). These compounds currently have no competitors in terms of hydrogen content. For example, volumetric density of hydrogen is 0.112 g/cm^3 in sodium borohydride and 0.145 g/cm^3 in ammonia borane. All these values exceed that of liquid hydrogen (0.07 g/cm^3). Furthermore, when hydrides react with water the hydrogen yield doubles due to reduction of protons from water [2].

Besides their high volume and mass H_2 capacity, another reason for the great attention paid lately to hydrides as compact forms of hydrogen storage is related to the easiness of hydrogen generation from them at ambient temperatures. In consideration of the variety of hydrides, the suitability of the candidate hydride was evaluated using the following selection criteria in addition to the maximum H_2 density [3]: the physicochemical state, storability, delivery manageability and reaction controllability, availability of the parent element, low environmental impact, recyclability, reaction heat and potential for economic feasibility. In the last years, sodium borohydride ($NaBH_4$) and ammonia-borane (NH_3BH_3) began to be seriously considered as potential sources of hydrogen [4,5]. Unlike most hydrides, these compounds do not require special storage conditions.

The analysis of the literature showed that catalytic systems based on Pt, Ru and Rh, including both bulk compounds and supported catalysts are the most active catalysts for hydrolysis of $NaBH_4$ and NH_3BH_3 [6–9]:

$$NaBH_4 + 2H_2O \rightarrow Na^+ + BO_2^- + 4H_2 \quad (1)$$

$$NH_3BH_3 + 2H_2O \rightarrow NH_4^+ + BO_2^- + 3H_2 \quad (2)$$

The use of supported catalysts is preferable because in this case there is no problem of catalyst separation from the reaction medium. Indeed, most scientific publications on $NaBH_4$ hydrolysis are devoted to investigation of supported catalysts of greatly varied chemical composition prepared by different methods Pt/TiO_2 and $Pt/LiCoO_2$ [10], $Pt/LiCoO_2$ and $Ru/LiCoO_2$ [11], bimetallic Pt-Pd/CNT [12], Ru/C [13,14], Pt/C [15–17], Ru/ZrO_2–SO_4^{2-} [18,19], Ru/Al_2O_3 [9], Ru/IRA [8,20], Rh/TiO_2 [21]. The data on supported catalysts used for hydrolysis of ammonia borane are scarce because it is studied only for the last 2–3 years. The analysis of the published data suggests that catalytic systems based on platinum group metals: Ru/Al_2O_3, Pt/Al_2O_3 and Rh/Al_2O_3 have the highest activity in this process as well [22–24].

* Corresponding author. Tel.: +7 3832 3307336; fax: +7 3832 3307336.
E-mail address: simagina@catalysis.ru (V.I. Simagina).

0920-5861/$ – see front matter © 2008 Elsevier B.V. All rights reserved.
doi:10.1016/j.cattod.2008.05.022

However, it should be noted that there are very few summarizing articles where a series of catalysts with different chemical composition were tested under the same conditions, the state of the active component was studied and the effects of the support, the active component precursor and catalyst preparation methods on the catalyst reactivity were analyzed. Also, despite the increasing interest to hydrolysis of hydrides, the effect of the properties of the active component formed directly in hydride solutions is not widely discussed in the literature.

In this study, we investigated several supported catalysts based on platinum group metals in hydrolysis of $NaBH_4$ and NH_3BH_3. Special attention was paid to the effect of the support on the catalyst reactivity. The catalysts reduction was carried out directly in hydride medium. The state of rhodium chloride on the surface of anatase TiO_2 and supported rhodium particles were studied by a complex of physicochemical methods.

2. Experimental

2.1. Catalyst preparation

"Sibunit" carbon material [25] having specific surface area (S_{BET}) of 530 m^2/g, γ-Al_2O_3 (JSC "Katalizator") with S_{BET} = 170 m^2/g, TiO_2 (anatase, Sigma–Aldrich) with S_{BET} = 243 m^2/g denoted as TiO_2-1 and industrial TiO_2 (JSC "Solikamsk Magnesium Plant") denoted as TiO_2-2 were used as powdered support samples. Specific surface area of TiO_2-2 was 74 m^2/g after calcination at 500 °C. The X-ray structural analysis showed that the major crystallographic form of TiO_2-2 was anatase (96%), the rutile content was 4%. The chemical analysis showed the presence of the following impurities: Nb, 0.04 wt.%; S, 0.03 wt.%; Fe, 0.22 wt.%; Ca, 0.58 wt.%.

Aqueous solutions of $RhCl_3{\cdot}nH_2O$, H_2PtCl_6 and $Ru(OH)Cl_3$ (JSC "AURAT") were used for preparation of the catalysts. After impregnation, the catalysts were dried in air for 2 h at 110–130 °C. The metal contents varied from 1 to 6 wt.%. In some cases, noted in the text Rh/TiO_2-2 catalysts were subjected to additional heat treatment in air at 300 °C for 4 h. The Rh black sample was obtained by reduction of rhodium chloride with a sodium borohydride solution and dried in air for 2 h at 110–130 °C.

2.2. Activity testing

Hydrogen generation was carried out at 40 °C in a glass temperature-controlled internal mixing reactor equipped with a magnetic stirrer at the 800 rpm stirring rate. A weighed amount of $NaBH_4$ (0.0465 g; 1.2 mmol; Acros Organics, 98%) or ammonia borane (0.0372 g; 1.2 mmol; JSC "AVIABOR", 99%) was placed into the reactor and dissolved in 10 ml of distilled water. A weighed amount of the catalyst was added and the volume of generated hydrogen was measured using a gas burette. The catalysts were reduced directly in the hydride solutions. After reaction the catalysts were separated from the reaction medium, washed with distilled water, dried at 110–130 °C for 2 h in air and investigated by physical methods.

2.3. Catalyst characterization

The specific surface areas (S_{BET}) of the supports were determined by thermal argon desorption.

The concentrations of impurities in TiO_2 were found using inductively coupled plasma atomic emission spectrometry on an Optima 4300 DV instrument. The analysis was performed after dissolving the TiO_2 sample in an acid mixture.

Rh and Cl contents in catalysts were detected by X-ray fluorescence analysis using VRA-30 analyzer with a Cr anode.

The diffraction patterns of TiO_2 sample were obtained using a URD-63 diffractometer with Cu Kα radiation. The coherent-scattering regions were calculated using the Scherrer equation based on the half-widths of the strongest diffraction peak (1 0 1) for anatase. Quantitative analysis of the individual crystalline phases in the samples was performed with the use of the PCW program [26].

High-resolution transmission electron microscopy (HRTEM) studies were carried out using JEM-2010 instrument with lattice resolution 1.4 Å and accelerating voltage 200 kV. Periodic images of lattice structures were analyzed using digital Fourier transformation. The samples were fixed on "holey" carbon films supported on copper grids and investigated with the electron microscope.

The diffuse-reflectance UV–vis (DR UV–vis) spectra were measured in air at room temperature using a Specord M-40 spectrometer with a standard diffuse-reflectance attachment. The absorption of the support was compensated while recording the spectra.

The XPS spectra were recorded using a VG ESCALAB HP electron spectrometer with non-monochromatic Al Kα irradiation ($h\nu$ = 1486.6 eV, 200 W). The spectrometer binding energy (E_b) scale was calibrated using the positions of core levels $Au4f_{7/2}$ (84.0 eV) and $Cu2p_{3/2}$ (932.6 eV). The samples were deposited on a conducting Scotch tape and studied without any pretreatment. The charging in the samples was taken into account using $Ti2p_{3/2}$ (458.6 eV) and C1s (284.8 eV) lines. The Rh/Cl molar ratio was estimated from the ratio of $Rh3d_{5/2}$ (309 eV) and $Cl2p_{3/2}$ (198 eV) peak intensities.

3. Results and discussion

In our previous work [21], it was shown that the rate of catalytic reactions depends on the active component and catalyst support. When platinum group metals (Pt, Rh, Ru, Pd) were supported by impregnation from chlorides on various supports (TiO_2, Al_2O_3, Sibunit) the catalytic activity in $NaBH_4$ hydrolysis reaction decreased in the following order: Rh > Ru ≈ Pt ≫ Pd (1 wt.%). These catalysts were reduced directly in the sodium borohydride solution. Rhodium supported on titania was shown to be the most active catalyst for sodium borohydride hydrolysis (Fig. 1). The activity of Rh/TiO_2-1 catalyst supported on finely dispersed pure anatase was higher than that of the catalyst supported on the industrial sample TiO_2-2.

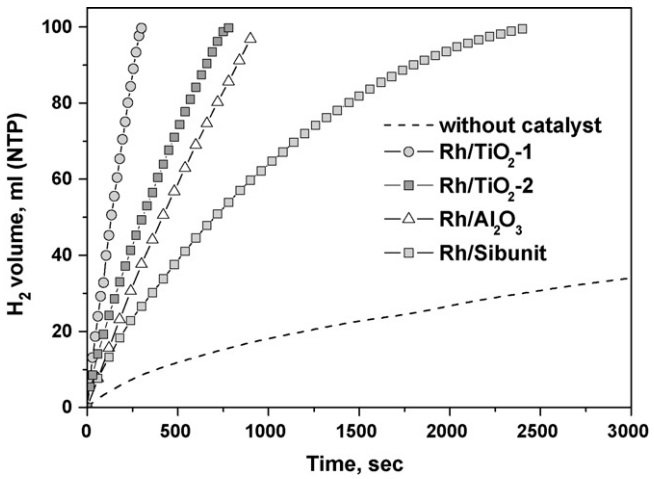

Fig. 1. H_2 generation from $NaBH_4$ solution at 40 °C over different supported catalysts with noble metal content 1 wt.%. The Rh:$NaBH_4$ molar ratio was 1:2000.

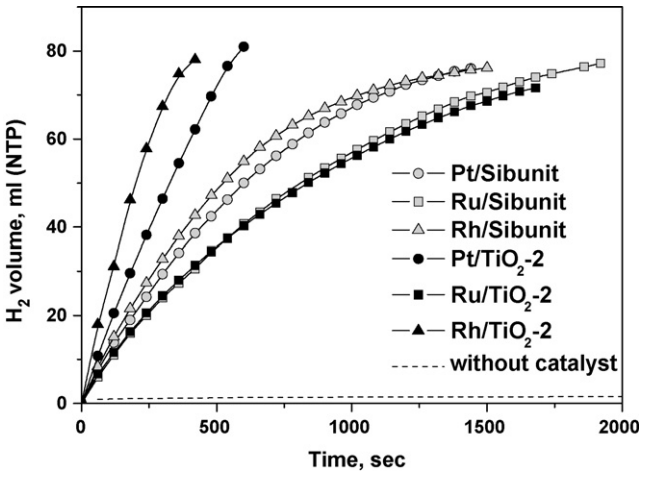

Fig. 2. H_2 generation from NH_3BH_3 solution at 40 °C over different supported catalysts with noble metal content 1 wt.%. The metal: NH_3BH_3 molar ratio was 1:2000.

Note that the obtained dependence is different from the activity order of the bulk metal chlorides. In the latter case, they are momentarily reduced, and the reactivity of the prepared metals goes down in the following order: Ru ≈ Rh > Pt ≫ Pd [27]. These differences can be related to the effect of the support on the properties of the metal clusters. These data contradict the results reported in an earlier paper [10], where Pd, Ru, Rh, Pt were deposited on titania by a different method—from acetylacetonates of the corresponding metals under supercritical conditions.

A similar dependence was also obtained for ammonia borane hydrolysis as well. Fig. 2 shows that the hydrogen generation rate from aqueous NH_3BH_3 solutions in the presence of supported catalysts grows in the order Ru < Pt < Rh. Rh/TiO_2 is the most active composition as in the case of sodium borohydride hydrolysis (Fig. 2). Note that a different reactivity order was obtained for NH_3BH_3 hydrolysis over catalysts supported on γ-Al_2O_3 with 2 wt.% concentration of the active component: Pd ≪ Ru < Rh ≤ Pt [22,23]. However, it should be mentioned that these catalysts were reduced in hydrogen before testing. Variation of the support showed the highest activity of platinum catalysts was observed when γ-Al_2O_3 was used as the support, the activity decreasing in the following order: Pt/γ-Al_2O_3 > Pt/C > Pt/SiO_2 [22,23].

Fig. 3 presents HRTEM images of Rh/TiO_2-2, Rh/γ-Al_2O_3 and Rh/Sibunit after testing in $NaBH_4$ hydrolysis and the image of rhodium black separated from the reaction mixture after testing of rhodium chloride. One can see that Rh black is formed from $RhCl_3$ after contact with $NaBH_4$. The Rh black sample consists of large loose aggregates with typical dimensions of tens of nanometers. These aggregates are composed from particles with the average size ca. 5 nm (Fig. 3d). The rhodium chloride deposition on the surface of a support favors stabilization of rhodium nanoparticles. As it is shown in Fig. 3a–c, the average sizes of supported rhodium metal particles formed on the Rh/TiO_2-2, Rh/Sibunit and Rh/γ-Al_2O_3 after reduction in $NaBH_4$ are 2.5, 3.2, and 3.2 nm, correspondingly. Despite similar sizes of rhodium particles formed on the surface of the studied supports, their reactivity is different (Fig. 1). We would like to note that earlier results on the effect of the dispersity of supported metal particles on their reactivity in hydrolysis of $NaBH_4$ and NH_3BH_3 are ambiguous [10,17,23].

Significant differences of the catalytic activity can be explained by changes of the active component properties under the influence of the support. This is most vividly demonstrated by the results presented in Fig. 4. One can see that the activity of rhodium

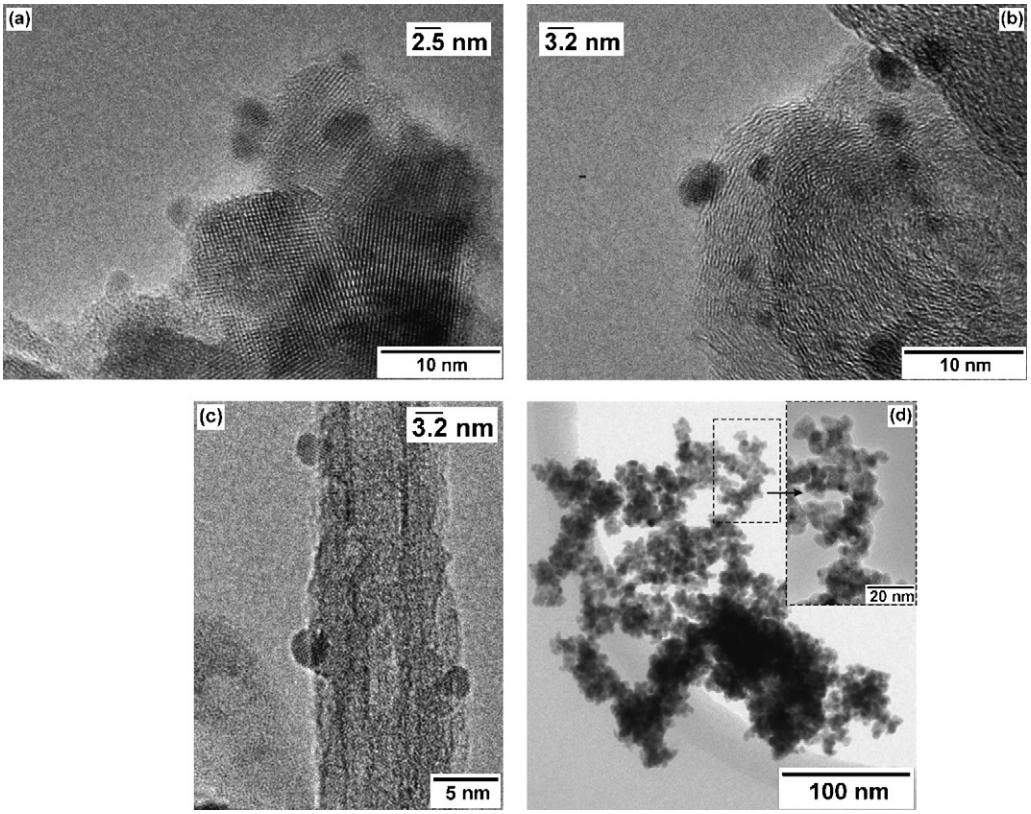

Fig. 3. TEM images of the catalysts tested in $NaBH_4$ hydrolysis: a, 1 wt.% Rh/TiO_2-2; b, 1 wt.% Rh/Sibunit; c, 1 wt.% Rh/Al_2O_3; d, Rh black. Catalysts were dried at temperature 110–130 °C.

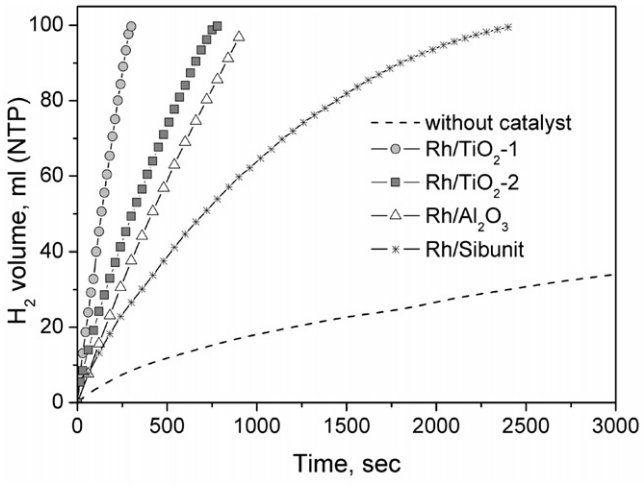

Fig. 4. H_2 generation from $NaBH_4$ solution at 40 °C over initial $RhCl_3{\cdot}nH_2O$, $RhCl_3{\cdot}nH_2O$ with the addition of a portion of TiO_2-1 (0.0061 g) and Rh/TiO_2-1 catalyst with 1 wt.% Rh. The Rh:$NaBH_4$ molar ratio was 1:2000.

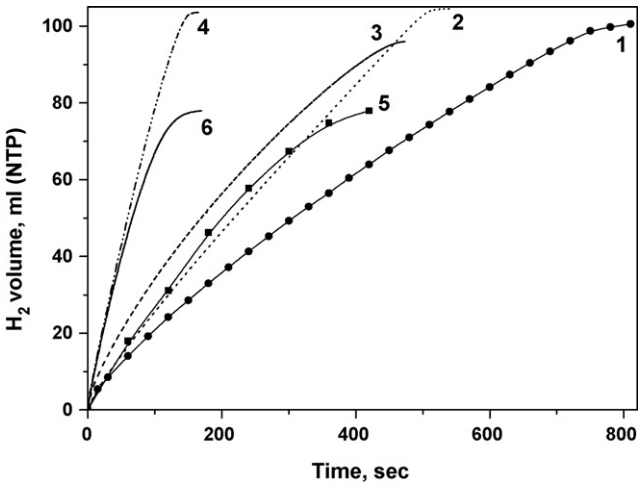

Fig. 6. H_2 generation from $NaBH_4$ (curves 1–4) and NH_3BH_3 (curves 5 and 6) solutions at 40 °C over Rh/TiO_2-2 catalysts with Rh content 1 wt.% (curves 1, 2 and 5) or 5.9 wt.% (curves 3, 4 and 6). Some catalysts were preliminary calcinated at 300 °C (curves 2 and 4), others—at 110–130 °C. Catalyst weight is 0.0062 g.

chloride deposited on titanium dioxide significantly exceeds that of bulk rhodium chloride. Also in the case of $RhCl_3$ the hydrogen generation rate considerably decreases with time, probably, due to aggregation of Rh^0 particles formed in the reaction with $NaBH_4$ (Fig. 3d). The addition of a titania sample into the reaction mixture together with the rhodium chloride solution makes it possible to increase the hydrogen generation rate, especially at long reaction times (Fig. 4). In this case, the rhodium metal particles formed in the solution are, most likely, stabilized on the TiO_2 surface to form more active sites for hydrolysis of sodium borohydride.

The effect of titanium dioxide on the electronic properties of rhodium particles formed in $NaBH_4$ is demonstrated by the XPS data. The XPS spectra of unreduced and reduced Rh/TiO_2 (5.9 wt.% Rh) are shown in Fig. 5a. The photoemission peak at 309.2 eV in the spectrum of unreduced catalyst can be assigned to $Rh3d_{5/2}$ that is typical for Rh^{3+} species [28]. The XPS spectrum of Rh black sample obtained by reduction of rhodium chloride by sodium borohydride shows a band at 307.1 eV. According to the literature [28], the band at 307.2 eV is attributed to Rh metal. The increase of the binding energy by 0.4 eV in the case of reduced Rh/TiO_2 may indicate that the rhodium metal particles are electron-deficient. Apparently, some rhodium is not reduced in the reaction medium due to its interaction with surface oxygen atoms of titania. It is known that when noble metal catalysts supported on oxides are reduced by hydrogen, some of the active component forms bonds with the oxygen atoms of the surface [29].

A shoulder at lower binding energies typical for Ti^{3+} appears in the Ti2p spectrum of the Rh/TiO_2 sample in comparison with the initial TiO_2 support (Fig. 5b). The difference spectrum indeed shows the presence of an additional Ti state with binding energy 457.6 eV. This value is close to that typical for Ti^{3+} [30]. Most likely, partial reduction of the support by $NaBH_4$ takes place.

Fig. 6 presents a comparison of the activities of Rh/TiO_2 catalysts with 1 and 5.9 wt.% Rh in hydrolysis of $NaBH_4$ and NH_3BH_3. When the rhodium concentration is increased from 1 to 5.9 wt.%, the hydrogen generation rate increases during hydrolysis of both sodium borohydride (curves 1 and 3) and ammonia borane (curves 5 and 6). NH_3BH_3 decomposes faster than $NaBH_4$. High hydrogen generation rate during sodium borohydride hydrolysis comparable with that observed in the case of ammonia borane was achieved when the temperature of the catalyst heat treatment in air was increased from 110–130 to 300 °C (curves 1, 2 and 3, 4).

One can expect that rhodium chloride interacts stronger with the support when the preliminary calcination temperature of the catalyst increases from 110–130 to 300 °C. Calcination at 300 °C is known to results in desorption of both weakly bound and strongly bound water from the surface of the support [31,32]. Probably, Rh^{3+} complexes can interact with the anatase surface sites that were previously blocked by water molecules.

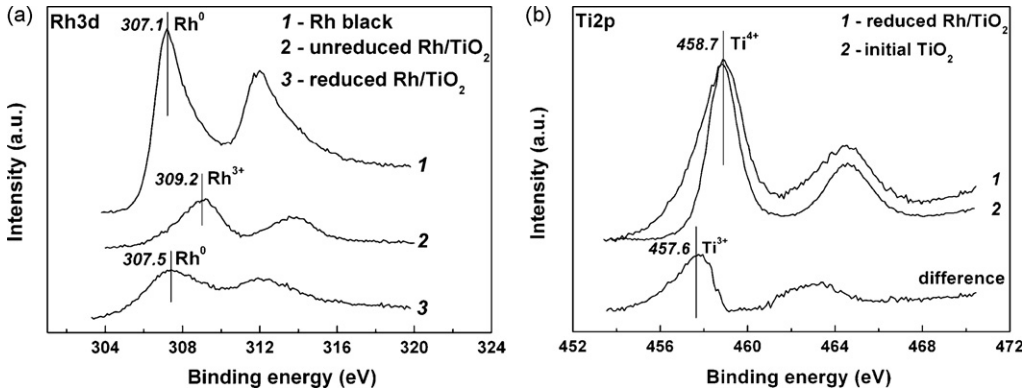

Fig. 5. XPS spectra of 5.9 wt.% Rh/TiO_2-2 catalysts (unreduced dried at 110–130 °C and reduced with $NaBH_4$), rhodium black and initial TiO_2: a, Rh3d photoelectron peaks; b, Ti2p photoelectron peaks.

Table 1
The Cl/Rh molar ratio for 5.9 wt.% Rh/TiO_2-2 catalyst calcined at different temperature

Temperature (°C)	Cl/Rh molar ratio	
	X-ray photoelectron spectroscopy	X-ray fluorescence analysis
110–130	2.8	2.8
300	1.8	2.2

To understand how the state of rhodium chloride deposited on the titania surface changes, the Rh/TiO_2 catalyst samples subjected to different thermal treatments in air were studied by various physical methods.

The XPS study of 5.9% Rh/TiO_2 samples calcined at different temperatures showed that the Cl/Rh molar ratio decreased with the temperature growth (Table 1). These results were confirmed by X-ray fluorescence analysis. Note that bulk rhodium chloride starts to react with oxygen from air only at 700–900 °C.

Fig. 7a shows the UV–vis diffuse-reflectance spectra of the initial compounds: titania (spectrum 1) and rhodium chloride (spectrum 2). Upon supporting $RhCl_3$ onto the titania surface, the position of the most intensive absorption band at 18,900 cm^{-1} shifted by 700 cm^{-1} to higher frequency (spectrum 1 in Fig. 7b; absorption band at 19,600 cm^{-1}). According to Lever [33], this absorption band can be attributed to d–d transitions in a hexacoordinated Rh^{3+} ion.

Along with the changes related to d–d transitions, a new band at 25,000 cm^{-1} was observed in the spectrum of unreduced Rh/TiO_2 catalysts. The shift of the absorption band at 18,900 cm^{-1} to higher frequency in the spectrum of $RhCl_3$ salt supported on TiO_2 and the appearance of a new absorption band at 25,000 cm^{-1} are evidently caused by partial substitution of chlorine for a stronger ligand—the surface oxygen with the formation of the Ti–O–Rh bond.

The attribution of band at 25,000 cm^{-1} to the Ti–O–Rh bond was reported by us earlier [21]. In that paper preliminary modification of the titania surface with sulfate ions was shown to result in blocking of its active sites and, as a consequence, significant weakening of this band in the spectrum of supported rhodium chloride. An absorption band close to 25,000 cm^{-1} was observed earlier during investigation of the interaction of transition and noble metal cations with the TiO_2 surface [34–37]. It was attributed to a charge transfer band between the metal ions and the support surface. Also it is well known that after deposition of various transition and noble metals on the anatase surface they form various surface compounds [38–40].

The analysis of the spectra shows that the calcination temperature increase from 110–130 to 300 °C results in a considerable growth of total absorption in the DR UV–Vis spectra and significant increase of the intensity of this absorption band (Fig. 7b). The growth of the intensity of the absorption band at 25,000 cm^{-1} when the calcination temperature is increased indicates that the effect of TiO_2 on the state of Rh^{3+} becomes stronger. Additional Ti–O–Rh bonds can be formed due to desorption of strongly bound water blocking the surface active sites and further substitution of some chlorine ions for oxygen anions belonging to the anatase surface.

According to the TEM data, the thermal treatment of the rhodium chloride sample supported on titanium dioxide has a significant effect on the state of rhodium particles forming due to reduction by sodium borohydride. According to the TEM data, the average size of metal nanoparticles in the reduced 5.9 wt.% Rh/TiO_2-2 sample preliminary dried at 110–130 °C was 3.5 nm (Fig. 8a). The rhodium particles were located on the surface of titanium dioxide in the form of groups. On the surface of the catalyst calcined at 300 °C, the metal nanoparticles were isolated from each other and their average size was 2.5 nm.

While discussing the data presented in Figs. 1 and 4, we showed that the size of supported rhodium particles formed directly in $NaBH_4$ is not the main factor determining the activity of the catalysts. Modification of the properties of rhodium particles after their deposition on different supports is a more important factor. It is natural to suppose that the change of the degree of rhodium chloride interaction with the TiO_2 surface due to the increase of the calcination temperature may also affect the properties of supported rhodium particles. The effect of the support on the properties of supported metal particles that are reduced by hydride at low temperature is practically not reported in the scientific literature and requires further detailed studies. On the contrary, the effect of strong metal-support interaction (SMSI) is extensively

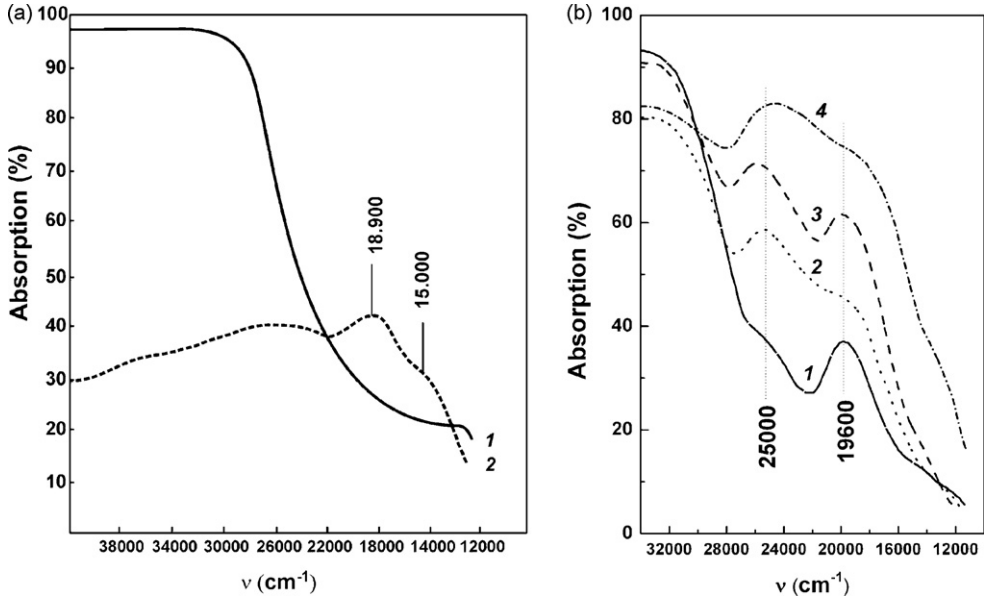

Fig. 7. DR UV-vis spectra: a, TiO_2-2 (curve 1) and $RhCl_3 \cdot nH_2O$ (curve 2); b, unreduced Rh/TiO_2-2 catalysts: (1) dried at 110–130 °C, 1 wt.% Rh; (2) calcined at 300, 1 wt.% Rh; (3) dried at 110–130 °C, 5.9 wt.% Rh; (4) calcined at 300, 5.9 wt.% Rh.

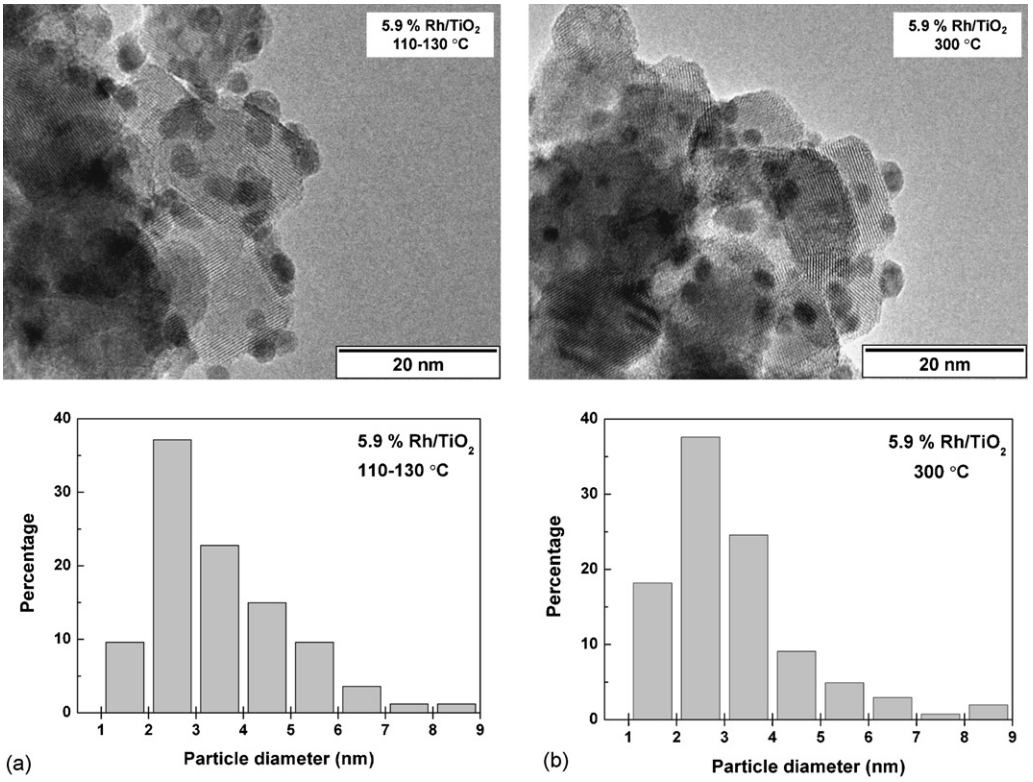

Fig. 8. TEM images and Rh nanoparticle size distribution of reduced 5.9 wt.% Rh/TiO_2-2 catalysts preliminary calcined at different temperatures: a, 110-130 °C; b, 300 °C.

studied for Rh/TiO_2 when hydrogen is used as the reducing agent [41].

4. Conclusions

Hydrogen generation from $NaBH_4$ and NH_3BH_3 hydrolysis has been studied over supported noble metal catalysts. Among Rh, Ru, Pt catalysts supported on "Sibunit" carbon material, γ-Al_2O_3 and TiO_2 with low metal concentration (1 wt.%), Rh/TiO_2 exhibits the highest activity in these processes. Despite similar dimensions of rhodium particles formed in the sodium borohydride solution on the supports surface, their reactivity is very different. Preliminary calcination of Rh/TiO_2 at 300 °C increases the catalyst activity in $NaBH_4$ hydrolysis. The results obtained by different physical methods (TEM, DRS UV–vis, and XPS) demonstrate the influence of the rhodium chloride interaction with titania on the properties of supported rhodium particles.

Acknowledgements

The authors are grateful to S.V. Tsybulya, N.N. Boldyreva, I.L. Kraevskaya and T.Yu. Volozhanina for assistance in the investigation of the catalysts.

References

[1] R.C. Weast (Ed.), CRC Handbook of Chemistry and Physics, 70th ed., CRC Press, Boca Raton, Florida, 1989.
[2] R.E. Davis, E. Bromels, C.L. Kibby, J. Am. Chem. Soc. 84 (1962) 885.
[3] V.C.Y. Kong, F.R. Foulkes, D.W. Kirk, J.T. Hinatsu, Int. J. Hydrogen Energy 24 (1999) 665.
[4] S.C. Amendola, S.L. Sharp-Goldman, M.S. Janjua, M.T. Kelly, P.J. Petillo, M. Binder, J. Power Sources 85 (2000) 186.
[5] F.H. Stephens, V. Pons, R.T. Baker, Dalton Trans. 25 (2007) 2613.
[6] M. Dasgupta, M.K. Mahanti, Trans. Met. Chem. 12 (1987) 433.
[7] M. Zahmakıran, S. Özkar, J. Mol. Catal. A: Chem. 258 (2006) 95.
[8] S.C. Amendola, S.L. Sharp-Goldman, M.S. Janjua, M.T. Kelly, P.J. Petillo, M. Binger, J. Power Sources 85 (2000) 186.
[9] D. Gervasio, S. Tasic, F. Zenhausern, J. Power Sources 149 (2005) 15.
[10] Y. Kojima, K. Suzuki, K. Fukumoto, M. Sasaki, T. Yamamoto, Y. Kawai, H. Hayashi, Int. J. Hydrogen Energy 27 (2002) 1029.
[11] Z. Liu, B. Guo, S.H. Chan, Ee Ho Tang, L. Hong, J. Power Sources 176 (2008) 306.
[12] R. Peña-Alonso, A. Sicurelli, E. Callone, G. Carturan, R. Raj, J. Power Sources 165 (2007) 315.
[13] B.S. Richardson, J.F. Birdwell, F.G. Pin, J.F. Jansen, R.F. Lind, J. Power Sources 145 (2005) 21.
[14] J.S. Zhang, W.N. Delgass, T.S. Fisher, J.P. Gore, J. Power Sources 164 (2007) 772.
[15] D. Xu, H. Zhang, W. Ye, Catal. Commun. 8 (2007) 1767.
[16] G. Guella, B. Patton, A. Miotello, J. Phys. Chem. C 111 (2007) 18744.
[17] C. Wu, H. Zhang, B. Yi, Catal. Today 93–95 (2004) 477.
[18] U.B. Demirci, F. Garin, Catal. Commun. 9 (2008) 1167.
[19] U.B. Demirci, F. Garin, J. Mol. Catal. A: Chem. 279 (2008) 57.
[20] S.C. Amendola, S.L. Sharp-Goldman, M.S. Janjua, N.C. Spencer, M.T. Kelly, P.J. Petillo, M. Binger, Int. J. Hydrogen Energy 25 (2000) 969.
[21] V.I. Simagina, P.A. Storozhenko, O.V. Netskina, O.V. Komova, G.V. Odegova, T.Yu. Samoilenko, A.G. Gentsler, Kinet. Catal. 48 (2007) 168.
[22] Q. Xu, M. Chandra, J. Alloys Compd. 446/447 (2007) 729.
[23] M. Chandra, Q. Xu, J. Power Sources 168 (2007) 135.
[24] M. Chandra, Q. Xu, J. Power Sources 156 (2006) 190.
[25] US Patent 4,978,649 (1990).
[26] W. Kraus, G. Nolze, PowderCell for Windows (version 2.3), Federal Institute for Materials Research and Testing, Berlin, Germany, 1999.
[27] H.C. Brown, C.A. Brown, J. Am. Chem. Soc. 84 (1962) 1493.
[28] J.F. Moulder, W.F. Stickle, P.E. Sobol, K.D. Bomben, Handbook of X-ray Photoelectron Spectroscopy, PerkinElmer Corporation, 1992.
[29] D.C. Koningsberger, J.H.A. Martens, R. Prins, D.R. Short, D.E. Sayers, J. Phys. Chem. 90 (1986) 3047.
[30] C.M. Chan, S. Trigwell, T. Duerig, Surf. Interface Anal. 15 (1990) 349.
[31] J. Nickl, D. Dutoit, A. Baiker, Appl. Catal. A: Gen. 98 (1993) 173.
[32] K.I. Hadjiivanov, D.G. Klissurski, A.A. Davydov, J. Catal. 116 (1989) 498.
[33] A.B.P. Lever, Inorganic Electronic Spectroscopy, Elsevier, Amsterdam, 1984, p. 554.
[34] O.V. Komova, A.V. Simakov, V.A. Rogov, D.I. Kochubei, G.V. Odegova, V.V. Kriventsov, E.A. Paukshtis, V.A. Ushakov, N.N. Sazonova, T.A. Nikoro, J. Mol. Catal. A: Chem. 161 (2000) 191.
[35] G.V. Odegova, E.M. Slavinskaya, Kinet. Catal. 45 (2004) 133.
[36] L.Ya. Mostovaya, N.A. Kovalenko, T.S. Petkevich, Yu.G. Egiazarov, J. Appl. Spectrosc. 60 (1994) 487.

[37] W. Choi, A. Termin, M.R. Hoffmann, J. Phys. Chem. 98 (1994) 13669.
[38] K. Bourikas, C. Kordulis, J. Vakros, A. Lycourghiotis, Adv. Colloid Interface Sci. 110 (2004) 97.
[39] G. Munuera, A.R. Gonzalez-Elipe, J.P. Espinos, A. Muñoz, J.C. Conesa, J. Soria, J. Sanz, Catal. Today 2 (1987) 663.
[40] K. Hadjiivanov, J.C. Lavalley, J. Lamotte, F. Maugé, J. Saint-Just, M. Che, J. Catal. 176 (1998) 415.
[41] S. Bernal, J.J. Calvino, M.A. Cauqui, J.M. Gatica, C. López Cartes, J.A. Pérez Omil, J.M. Pintado, Catal. Today 77 (2003) 385.